Mem. S.A.It. Vol. 75, 470

Memorie della

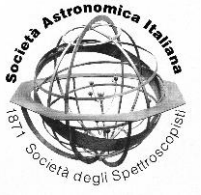

Geminga: a tale of two tails, and much more

P.A. Caraveo[1], G.F. Bignami[2,3], A. De Luca[1,4], A. Pellizzoni[1], S. Mereghetti[1], R.P. Mignani[5], A. Tur[2], W. Becker[6]

[1] INAF/IASF "G. Occhialini", Via Bassini 15, 20133 Milano, Italy e-mail: pat@mi.iasf.cnr.it
[2] Centre d'Etude Spatiale des Rayonnements, CNRS-UPS, 9, Avenue du Colonel Roche, 31028, Toulouse Cedex 4, France
[3] Università degli Studi di Pavia, Dipartimento di Fisica Nucleare e Teorica, Via Bassi 6, 27100 Pavia, Italy
[4] Università di Milano Bicocca, Dipartimento di Fisica, P.za della Scienza 3, 20126 Milano, Italy
[5] ESO, Karl Schwarzschild Strasse 2, D-85740, Garching bei München, Germany
[6] Max-Plank Institut für Extraterrestrische Physik, 85741 Garching bei München, Germany

Abstract. We report on the deep (100 ksec) *XMM-Newton* EPIC observation of the field of the Geminga pulsar. The unprecedented throughput of the instrument allowed to detect two elongated parallel x-ray tails trailing the neutron star. They are aligned with the object's supersonic motion, extend for ∼2', and have a nonthermal spectrum produced by electron-synchrotron emission in the bow shock between the pulsar wind and the surrounding medium. Electron lifetime against synchrotron cooling matches the source transit time over the x-ray features' length. Such an x-ray detection of a pulsar bow shock allows us to gauge the pulsar electron injection energy and the shock magnetic field while constraining the angle of Geminga's motion and the local matter density. We give also preliminary results on the timing and spectral analysis of the ∼63,000 photons collected from the neutron star.

Key words. Pulsars: individual (Geminga) – Stars: neutron – X-ray: stars – X-ray: ISM

1. Introduction

Geminga is a nearby, middle-aged isolated neutron star (Bignami & Caraveo 1996). Proximity is a key-parameter for understanding the multiwavelength behaviour of this source discovered in high-energy gamma-rays and later identified in X-rays (Bignami et al. 1983) and optical wavelengths (Bignami, Caraveo & Paul 1988).

Send offprint requests to: P.A. Caraveo

The smoking gun, confirming the previous work based on the interpretation of positional coincidence, came with the ROSAT discovery of a 237 msec periodicity (Halpern & Holt 1992), immediately seen also at higher energy in contemporary EGRET data (Bertsch et al. 1992) as well as in COS-B archival data (Bignami & Caraveo 1992). At the same time, significant proper motion was discovered at optical wavelengths (Bignami, Caraveo & Mereghetti 1993), definitely linking the pro-

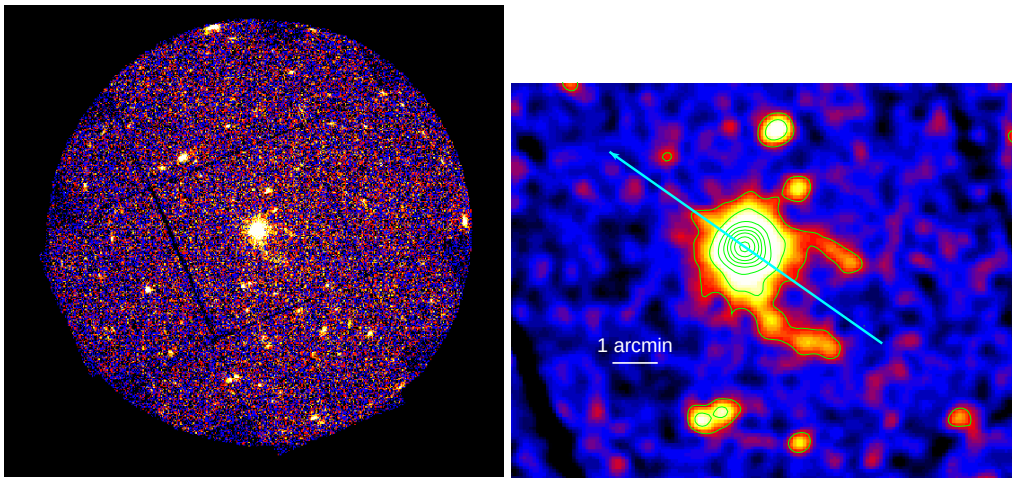

Fig. 1. (left) The *XMM-Newton* view of the field of Geminga. Data from the MOS1 and MOS2 cameras have been merged to produce the image. Events in the 0.3-5 keV range have been selected. The exposure time is of ∼ 77 ksec per camera. Geminga is the bright source close to the center of the image; the tails can be seen as two faint diffuse emission patterns emerging from the source. Many (∼ 100) serendipitous sources are also visible in the field. (right) Inner part of the field, shown after gaussian smoothing. The emission from Geminga outshines the tails up to ∼ 40″ from the source. The tails are ∼2 arcmin long and cover an area of ∼2 square arcmin. They show a remarkable symmetry with respect to the pulsar proper motion direction, marked by the arrow.

posed counterpart to a fast-moving, pulsar-like object, the distance to which was later nailed down to 160 pc through its optical parallax (Caraveo et al. 1996). Thus, Geminga qualifies as a pulsar, and as such is listed in the pulsar catalogue[1], although it has not been detected at radio wavelengths. Indeed, the absence of a radio signal prompted Caraveo, Bignami & Trumper (1996) to use this source as the prototype of a new class of pulsars: the radio-quiet ones, now encompassing the so called "dim sources" (Treves et al. 2000), the CCO (Pavlov et al. 2002), the next Geminga(Halpern et al. 2002) and other potential candidates, including a number of proposed counterparts of EGRET sources. Gamma-ray emission is not a common characteristics of these radio quiet INSs. Rather, their common denominator is their thermal soft X-ray emission coupled with very faint (if any) optical radiation. Here we report on the *XMM-Newton* EPIC data ofa long Geminga exposure which almost triples the number of soft photons available from this source. Such improved statistics allows to study the object's light curve as a function of the photon energy. The total (average) source spectral shape can be assessed using three independent instruments, while the time-tagging of photons allows, for the first time, to follow the evolution of the source spectral shape as a function of phase.

2. The EPIC data

XMM-Newton performed a 100 ksec exposure on Geminga on April 4th, 2002. While the two MOS EPIC cameras were operated with the medium filter in their "full frame" mode (Turner et al. 2001) the pn camera was operated with the thin filter in "small window" mode to allow for accurate timing of source photons (Strüder et al. 2001). Data were

[1] http://www.atnf.csiro.au/research/pulsar/psrcat/

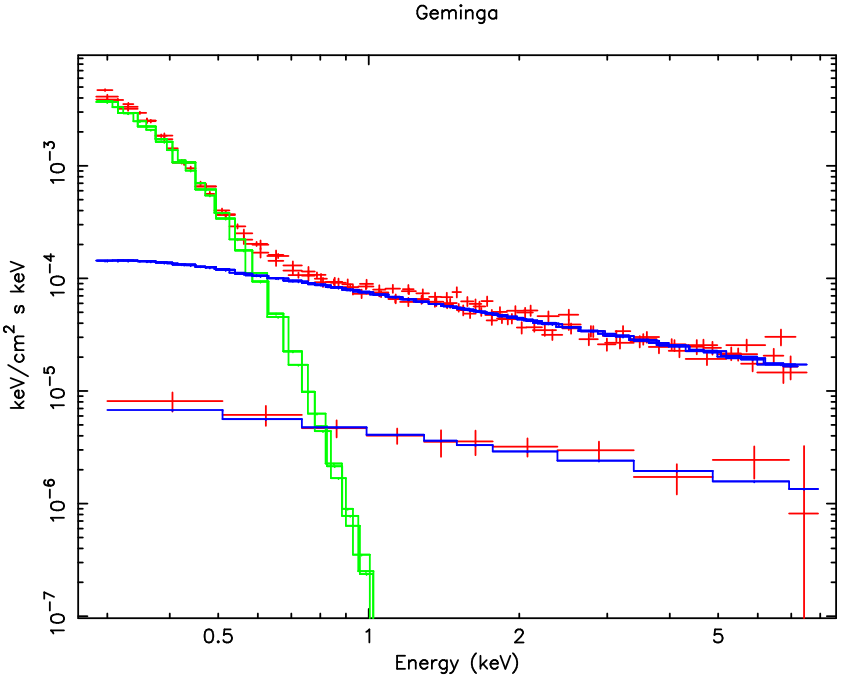

Fig. 2. Unfolded spectrum of Geminga (upper curve) and its tails (lower curve). The spectrum of the pulsar (pn, MOS1 and MOS2 data points are plotted together) is well reproduced by the sum of a blackbody function and a hard power law (see text). The spectrum of the tails (the sum of MOS1 and MOS2 data is plotted) is also well described by a similar hard power-law curve.

processed with the XMM Newton Science Analysis Software (SAS version 5.4.1). After removing time intervals with high particle background and correcting for the dead time, we obtain a net exposure time of 55.0 ksec for the pn camera and 76.9 and 77.4 ksec for the MOS1 and MOS2, respectively. The Geminga count rates (0.2<E<7 keV) are 0.807±0.004 counts s^{-1} for the pn and 0.119±0.001 counts s^{-1} and 0.123±0.001 counts s^{-1} for the MOS1 and MOS2, respectively. The sum of the MOS1 and MOS2 images is shown in Figure 1. Besides Geminga, which shines at the center of the image, more than 100 serendipitous sources have been detected. Identification work is in progress on such sources and will be reported elsewhere. For a thorough discussion of the "tails", which are seen by EPIC for the first time as trailing Gemingaand well aligned with the source proper motion, the reader is referred to Caraveo et al. (2003). Briefly, we recall here the most important characteristics of this newly-discovered X-ray feature of Geminga.

The tails are two patterns of diffuse emission, originating close to Geminga (they cannot be resolved in proximity of the bright point source closer than 40″ at most) and extending up to ∼ 3 arcmin away from the pulsar, well aligned with the NS proper motion, with a thickness of ∼ 20″ − 30″. Their spectrum is well reproduced by a slightly absorbed ($N_H \sim 10^{20}\ cm^{-2}$) power law with photon index $\Gamma \sim 1.6$. At the pulsar distance (160 parsecs), their unabsorbed 0.3-5 keV flux corresponds to a luminosity of 6.5×10^{28} erg s^{-1} ($\sim 2 \times 10^{-6}$ of Geminga's rotational energy loss). Possible contributions from point sources are estimated to be negligible.

The shape of the tails is reminiscent of the projection on the plane of the sky of an empty paraboloid of X-ray emission, the edges

of which show up brighter because of a limb effect. Such a morphology is naturally explained in terms of a bow-shock formed between the pulsar relativistic wind and the dynamical pressure generated by its supersonic motion through the interstellar medium.

The hard, power-law spectrum of the tails can be explained by synchrotron emission of high-energy electrons accelerated by the pulsar, girating in the shocked interstellar magnetic field. Such an interpretation provides a direct gauge of the pulsar wind injection energy, demonstrating that Geminga accelerates electrons up to 10^{14} eV, a value very close to the upper limits expected on the basis of the pulsar's energetics, allowing also to constrain the local interstellar magnetic field in the range 2-3 μG. The Larmor radius of the emitting electrons in the bow-shock magnetic field ($\sim$ 27″ at the distance of Geminga) is found to be in excellent agreement with the observed thickness of the tails. Moreover, electron lifetime against synchrotron emission ($\sim$ 800 years) matches the pulsar transit time over the X-ray features' length ($\sim$ 1000 years, on the basis of the well known proper motion of Geminga), supplying a final, independent consistency check to our model.

The observed geometry of the tails, compared to a 3-D bow-shock model assuming a spherical pulsar wind in an homogeneous ISM, allows also to constrain the angle of the source motion with respect to the plane of the sky to be less than $\sim$ 30°, and therefore to assess its 3-D space velocity. The detection of the pulsar bow-shock represents also an important way to probe the interstellar medium, constraining its density to be in the range 0.06-0.15 atoms cm^{-3}, in good agreement with the expected value of the ISM density for the region around Geminga (Gehrels & Chen 1993).

The good EPIC statistics allows for an accurate spectrum to be drawn, for the first time, of both the pulsar and its tails, in the range 0.2 to ~7 keV. Fig. 2 shows such time-averaged spectrum of both the pulsar (upper curve) and its surrounding diffuse emission, drawn on the source energy flux scale. Note that the upper curve plots both the pn and the 2 MOS data (superimposed and undistinguishable), while the lower curve for the extended emission (tails) contains MOS data only, since the pn camera was used in "small window" mode. While a more detailed interpretation of the source physics as portrayed by Fig. 2 will be the topic of an upcoming work, we propose here a few qualitative, obvious comments. The point-source spectrum (upper curve) shows with a striking clarity that two different mechanisms are at work. Below $\sim$ 0.7 keV, the emission is undoubtely thermal, well fit by a temperature of ~43 eV, implying an emitting surface of $\sim$ 9 km at 160 parsec. For the whole energy decade 0.7-7 keV, Geminga's spectrum is equally well fit by a single power law, with photon index α ~1.85. The simplest interpretation of such hard power law (already suggested by the ROSAT data of Halpern & Holt, 1992) is that of synchrotron emission by energetic electrons radiating in the pulsar magnetic field.

For the diffuse emission from the tails (lower curve of Fig. 2) a striking similarity is apparent with the hard spectral shape of the point source. This points to a similar physical origin between the source and the tails hard X-ray photons. The latter, however, must necessarily be created by the high energy (10^{14} eV) end of the pulsar electron spectrum, since they radiate in the compressed IS magnetic field of $\sim 10^{-5}$ G.

3. Timing analysis

Exploiting the much improved EPIC energy resolution with respect to both ASCA and ROSAT, our data allow, for the first time, to render apparent the pulsar light curve morphology variation as a function of photon energy.

Fig. 3 shows such energy-resolved time curves for four different energy ranges: 0.15-0.35, 0.35-0.7, 0.7-2.0 and 2.0-6.0 keV. The light curve morphology variation is apparent. The lower energy, thermal emission has a smooth light curve featuring a single, wide peak. At high energy, two peaks are present during each phase interval, separated by ~0.4 phase. It is, at the moment, not possible to relate in absolute phase the EPIC X-ray peaks to the EGRET γ-ray peaks; however, we note the striking similarity between the two non-

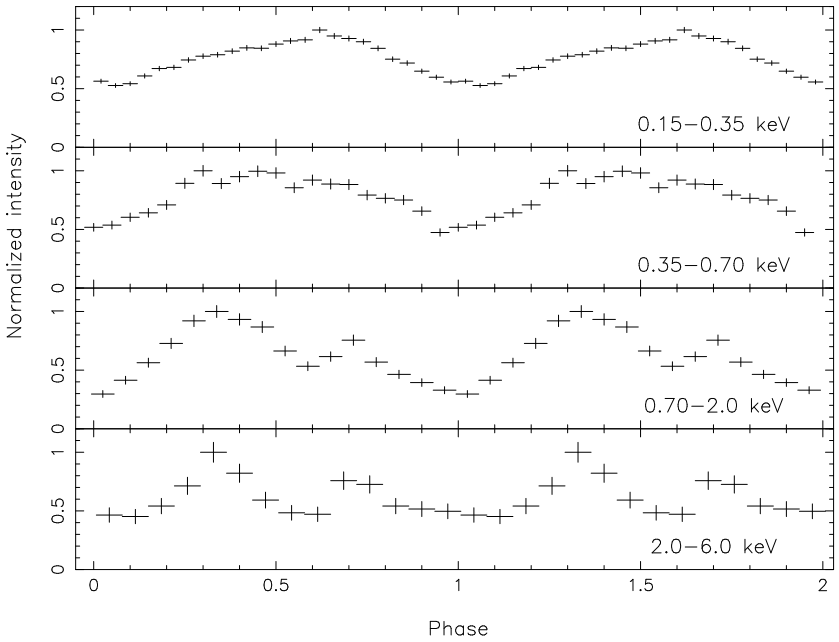

Fig. 3. Folded light curves of Geminga in different energy ranges. Morphology variations of the pulse profile as a function of energy are clearly evident (see text).

thermal light curves of the same object. A phase shift of about 0.3 phase is also obviously present between the single peak of the thermal emission and the highest of the two non-thermal peaks. As expected, the "intermediate" energy range (0.35 to 0.7 keV) shows a somewhat mixed behaviour due to the symultaneous presence of the two components. Such components are obviously of very different physical origin, also possibly in terms of production zone. Finally, we note that the pulsed fraction of the radiation as a function of energy does not seem to show the spectacular variation proposed by Jackson et al. (2002) on the basis of ASCA data. In particular, the EPIC data do not confirm a pulsed fraction as high as, e.g., 80% or greater at high energy (E>4 keV). A final analysis of all aspects of light curve morphology variation with energy is currently in progress and will be published elsewhere.

4. An EPIC remark

The EPIC observation yielded a total of 63,000 photons. The vast majority ofthe EPIC harvest is due to the pn detector with 44,400 photon with the MOS1 and MOS2 detectors contributing 9,150 and 9520 photons respectively. The tails, which are made up by few hundreds photons, are not included in this budget. When compared with the 27,000 soft X-ray photons gathered during the ROSAT lifetime in the energy range (0.1-2.4 keV) and the 6,500 collected by ASCA in the energy range (0.7-8 keV), our EPIC observations stands out for its much improved statistics. Since the part of the spectrum benifitting most from the high troughput of the *XMM-Newton* telescope is the "high energy" one, it comes as no surprise that the EPIC spectrum constrain much better the high energy part of the source spectrum as well as its time-resolved behaviour.

References

Bertsch, D. L. et al. 1992, Nature, 357, 306
Bignami, G. F. & Caraveo, P. A. 1992, Nature, 357, 287

Bignami G.F. & Caraveo P.A., 1996, ARA&A, 34, 331
Bignami G. F., Caraveo P. A., & Lamb R. C., 1983, ApJL, 272, L9
Bignami, G. F., Caraveo, P. A., & Mereghetti, S. 1993, Nature, 361, 704
Bignami, G. F., Caraveo, P. A., & Paul, J. A. 1988, A&A, 202, L1
Caraveo, P. A., Bignami, G. F., DeLuca, A., Mereghetti, S., Pellizzoni, A., Mignani, R., Tur, A., & Becker, W. 2003, Science, 301, 1345
Caraveo, P. A., Bignami, G. F., Mignani, R., & Taff, L. G. 1996, ApJ, 461, L91
Caraveo, P. A., Bignami, G. F., & Trumper, J. E. 1996b, A&A Rev., 7, 209
Gehrels, N. & Chen, W. 1993, Nature, 361, 706
Halpern, J. P., Gotthelf, E. V., Mirabal, N., & Camilo, F. 2002, ApJ, 573, L41
Halpern, J. P. & Holt, S. S. 1992, Nature, 357, 222
Jackson, M. S., Halpern, J. P., Gotthelf, E. V., & Mattox, J. R. 2002, ApJ, 578, 935
Pavlov, G. G., Sanwal, D., Garmire, G. P., & Zavlin, V. E. 2002, ASP Conf. Ser. 271: Neutron Stars in Supernova Remnants, 247
Strüder, L. et al. 2001, A&A, 365, L18
Taylor, J. H., Manchester, R. N., & Lyne, A. G. 1993, ApJS, 88, 529
Treves, A., Turolla, R., Zane, S., & Colpi, M. 2000, PASP, 112, 297
Turner, M. J. L. et al. 2001, A&A, 365, L27